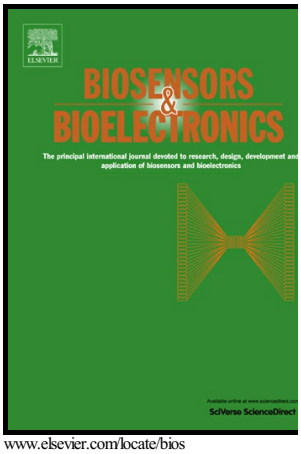

www.elsevier.com/locate/bios

TiO_2 nanoparticle modified organ-like Ti_3C_2 MXene nanocomposite encapsulating hemoglobin for a mediator-free biosensor with excellent performances

Fen Wang, ChenHui Yang, Max Duan, Yi Tang, JianFeng Zhu

PII: S0956-5663(15)30330-4
DOI: http://dx.doi.org/10.1016/j.bios.2015.08.004
Reference: BIOS7900

To appear in: *Biosensors and Bioelectronic*

Received date: 26 May 2015
Revised date: 1 August 2015
Accepted date: 3 August 2015

Cite this article as: Fen Wang, ChenHui Yang, Max Duan, Yi Tang and JianFeng Zhu, TiO_2 nanoparticle modified organ-like Ti_3C_2 MXene nanocomposit encapsulating hemoglobin for a mediator-free biosensor with excellen performances, *Biosensors and Bioelectronic* http://dx.doi.org/10.1016/j.bios.2015.08.004

TiO_2 nanoparticle modified organ-like Ti_3C_2 MXene nanocomposite encapsulating hemoglobin for a mediator-free biosensor with excellent performances

Fen Wang[1,*], ChenHui Yang[1,*], Max Duan[1], Yi Tang, JianFeng Zhu

Key Laboratory of Auxiliary Chemistry & Technology for Chemical Industry, Ministry of Education, Shaanxi University of Science & Technology, Xi'an, 710021, P.R. China.

Abstract

TiO_2 nanoparticle modified organ-like Ti_3C_2 MXene (TiO_2-Ti_3C_2) nanocomposite has been synthesised and then used to immobilize hemoglobin (Hb) to fabricate a mediator-free biosensor. The morphology and structure of TiO_2-Ti_3C_2 nanocomposite were characterized by scanning electron microscopy (SEM) and X-ray diffraction (XRD). Spectroscopic and electrochemical results revealed that TiO_2-Ti_3C_2 nanocomposite is an excellent immobilization matrix with biocompatibility for redox protein, affording good protein bioactivity and stability. Due to the special organ-like hybrid structure of TiO_2-Ti_3C_2, the direct electron transfer of Hb is facilitated and the prepared biosensors displayed good performance for the detection of H_2O_2 with a wide linear range of 0.1-380 μM for H_2O_2 (sensitivity of 447.3 μA mM^{-1} cm^{-2}), an extremely low detection limit of 14 nM for H_2O_2. Especially, numerous TiO_2 nanoparticles with excellent biocompatibility on the surface of the nanocomposite may provide a protective microenvironment for Hb to make the prepared biosensor improve long-term stability. The TiO_2-Ti_3C_2 based biosensor retains 94.6% of the initial response to H_2O_2 after 60-day

* Corresponding author: Tel.: +8615191434454; fax: +8602986168688.
E-mail address: ych488@163.com (C. Yang), wangf@sust.edu.cn (F. Wang).
[1] These authors contributed equally to this work.

storage. TiO_2-Ti_3C_2 nanocomposite could be a promising matrix for the fabrication of mediator-free biosensors, and might find wide potential applications in environmental analysis and biomedical detection.

Keywords: MXene; TiO_2; Direct electrochemistry; Biosensor; Long-term stability.

1. Introduction

To accomplish the direct electron transfer (DET) between the enzyme and the electrode is of great importance in fabrication of mediator-free electrochemical biosensors (Wang et al., 2010). Because the redox-active center of proteins is embedded in its protein shell deeply, the DET between the protein and the electrode surface is generally difficult (Armstrong et al., 1988; Heller, 1990; Hong et al., 2006; Lu et al., 2006; Lu et al., 2008; Scheller et al., 2005). Moreover, the enzyme usually loses its bioactivity that adsorbed directly onto the electrode surface (Hong et al., 2006; Wang et al., 2010). These problems make it difficult to transfer electrons directly at traditional electrodes (Wang et al., 2010). Therefore, to employ nano-materials is an efficient way to facilitate the direct electron transfer and retain the bioactivity of immobilized enzymes (Jin et al., 2007; Ma et al., 2009; Qiu et al., 2010). And among them, two-dimensional layered nano-materials, such as graphene (Elahi et al., 2014; Jain et al., 2013; Li et al., 2008; Wang et al., 2009) and MoS_2 (Xiao et al., 2010), have attracted extensive attention to being used for immobilization of biomolecules onto electrode surface, due to large specific surface areas, excellent electronic transport properties, and good biocompatibility.

MXenes are known that the constellation of 2D materials has been augmented by a new, and potentially quite large, group of early transition metal carbides and/or carbonitrides (Naguib et al., 2014). And they have stimulated research enthusiasm, because they combine hydrophilic surfaces, good structural and chemical stabilities, excellent electrical conductivities, and environment-friendly characteristics (Peng et al., 2014). Recently, we firstly reported on the layered transition metal carbide (MXene-Ti_3C_2) as the immobilization matrix for redox protein for biosensor (Wang et al., 2015). It is well-known that TiO_2 possesses superior biocompatibility and chemical stabilities (Xie et al., 2011; Xie et al., 2007; Zhang et al., 2007). To further improve biocompatibility of Ti_3C_2 (MXene), we select TiO_2 to modify Ti_3C_2 to afford protein bioactivity and stability more effectively.

Herein, TiO_2 nanoparticle modified Ti_3C_2 nanocomposite was synthesized by a simple in situ hydrolysis followed by a hydrothermal process. Just as schematic shows in Fig. 1, numerous TiO_2 nanoparticles loaded on the Ti_3C_2 layers substrate with an organ-like structure makes it possible for the nanocomposite to offer a number of advantages when it is used as a support for enzyme immobilization. The organ-like structure with one end closing of the Ti_3C_2 nano-layers and the other end opening of that is available for enzyme entrapment. The enzyme is funneled toward the interior among the Ti_3C_2 nano-layers and can become immobilized on the inner surfaces of the organ-like structure. Furthermore, TiO_2 nanoparticles with excellent biocompatibility may provide a protective microenvironment for the enzymes to retain their enzymatic stability and activity for long time. The nanoscaled TiO_2 (less than 30 nm in size) can greatly enhance the active surface area available for protein adsorption. Meanwhile the

substrate can simply be entrapped by the hybrid structure with high specific surface area, permitting the access of a large quantity of enzymes immobilized on the nanocomposite. The concentrated substrate and enzyme in this confined region will increase the effective collisions between them (Xie et al., 2011). Ti_3C_2 with excellent mobility of charge carriers can also become the excellent media of efficient electrical communication between the enzyme and the electrode. Hence, TiO_2 nanoparticle modified Ti_3C_2 nanocomposite is a promising support for enzyme immobilization and have potential applications in biosensors.

In this paper, using hemoglobin (Hb) as a model protein, the constructed TiO_2-Ti_3C_2 based mediator-free biosensor displayed good performance for the detection of H_2O_2 with wide linear range, low detection limit, and especially excellent long-term stability. Therefore, the present work can offer a new avenue to broaden the applications of MXenes in electrochemical biosensors.

2. Experimental

2.1. Materials and apparatus

Hb (from bovine blood) and Nafion solution (5 wt% in lower aliphatic alcohols) were purchased from Sigma. Unless otherwise noted, all other chemicals (analytical grade) were purchased from Sinopharm Chemical Reagent Co., Ltd., China. In all experiments deionized water was used.

Field-emission scanning electron microscopy (FE-SEM) was performed using a Hitachi S-4800 & Hiroba energy dispersive X-ray electron miscroscope. Specific surface area (SSA) was carried out the accelerated surface area and porosimetry system (ASAP 2460, Micromeritics Instrument Corporation,

Norcross (Atlanta), Georgia, USA). X-ray diffraction (XRD) patterns were recorded on a Rigaku D/max 2200pc diffractometer using Cu Kα radiation of wavelength λ= 0.15418 nm at 40 kV and 40 mA. FT-IR spectra were obtained on a Bruker TENSOR27 instrument. UV-vis spectra were recorded using a PerkinElmer Lambda-950 spectrophotometer. All electrochemical experiments were performed with a CHI 660E electrochemical workstation (CH Instruments, Shanghai, China). A conventional three-electrode system, which consisted of a platinum wire as the counter electrode, an Ag/AgCl/3M KCl as the reference electrode and a 3-mm diameter modified glassy carbon electrode (GCE) as the working electrode, was used in all electrochemical experiments. Unless otherwise noted, 0.1 M phosphate buffered saline (PBS; pH 7.0) was used as the supporting electrolyte in all experiments. The buffer was purged with highly purified nitrogen for at least 30 min and a nitrogen atmosphere environment was kept in electrochemical measurements.

2.2. Synthesis of TiO_2-Ti_3C_2 nanocomposite

Synthesis of Ti_3AlC_2. The MAX phase used as precursor for MXene synthesis herein—Ti_3AlC_2—was prepared by vacuum pressureless sintering method with mixing all powders of TiC (particle size < 75 μm, 99.5% purity), Ti (particle size < 50 μm, 99.5% purity), and Al (particle size < 75 μm, 99.5% purity) in a 2:1:1.2 molar ratio. The powders were ball-milled for 1 h at a speed of 900 rpm. Afterward, the mixture was sintered at 1350 °C for 2 h in vacuum (less than 4.0×10^{-2} Pa). The sintered product was high-energy ball milled in absolute ethyl alcohol for 2 h and dried at 50 ºC for 24 hours to obtain powders for further study. In all cases, the milled powder was sieved through a 400 mesh screen such

that the initial particle size was <38 μm. Fig. S1 and Fig. S2 give the SEM image and XRD pattern of Ti_3AlC_2.

Synthesis of Ti_3C_2 MXene. Ti_3C_2 was successfully prepared by etching Al from Ti_3AlC_2 in HF at room temperature. Firstly, 5.0 g as-prepared Ti_3AlC_2 powders were immersed in 80 mL 40% HF solution under magnetic stirring at room temperature for 48 h. Then the resulting MXene suspension was repeatedly washed 6 times using deionized water and centrifuged to separate the powder at 4000 rpm until the pH value of the liquid reached ~ 6. After decantation, the resulting powder was washed for 3 times by absolute ethanol and centrifuged to separate the powder, and left to dry in air at RT for 3 days. Finally, the powder was dried in the vacuum oven (< 0.09 MPa) at 50 °C for 24 hours. Fig. 1(a), Fig. S1(b) and Fig. S2 give the SEM images and XRD pattern of Ti_3C_2 MXene.

Synthesis of TiO_2-Ti_3C_2 nanocomposite. In a typical preparation of TiO_2-Ti_3C_2 nanocomposite, 150 mg of Ti_3C_2 was dispersed in 200 mL ethanol under magnetic stirring at room temperature for 1 h to get a homogenous suspension of Ti_3C_2. The suspension was mixed 0.5 mL of 0.4 mM KCl and was then stirred for 20 min. Next, 1.0 mL of tetrabutyl titanate (TBOT) was added to the mixture and was then stirred for 6 h in a dry atmosphere. At the end of the reaction, a gray precipitate was collected by centrifugation and rinsed sequentially with ethanol for 6 times and deionized water for 3 times. Then the precipitate was dispersed in 60 mL ethanol under stirring. After 15 min, the suspension was loaded in a 100 mL Teflon-lined autoclave. Then the autoclave was sealed and heated in an MDS-8 microwave hydrothermal system at 180 °C for 60 min. The nanocomposite (TiO_2-Ti_3C_2) was then collected,

washed with ethanol for 3 times and pure water for 3 times to remove ions and possible remnants. It was then dried at 50°C. Meanwhile, individual TiO_2 and Ti_3C_2 for control were synthesized separately following the same procedure. Fig. S3 gives the SEM image of TiO_2.

2.3. Preparation of enzyme electrode

To investigate the electrochemical behavior of TiO_2-Ti_3C_2 nanocomposite in the H_2O_2 biosensor, enzyme electrode was assembled. Prior to use, a glassy carbon electrode (GCE) was polished with 0.3 and 0.05 μm alumina slurry, and sonicated in ethanol and water successively. The cleaned GCE was dried using a purified nitrogen stream. The enzyme electrode was prepared by a simple casting method. Firstly, 1 mL of 2 mg mL^{-1} TiO_2-Ti_3C_2 suspension and 0.5 mL of 10 mg mL^{-1} Hb PBS were mixed and stirred for 20 min. Next, 0.5 mL of Nafion (5%) was added to the mixture and then stirred for 10 min. Finally, 4 μL of the mixture was applied to the surface of a freshly polished GCE to prepare the Nafion/Hb/TiO_2-Ti_3C_2/GCE and then stored in refrigerator at 4 °C prior to use.

In order to comparison, TiO_2 and Ti_3C_2 were used for the fabrication of Nafion/Hb/TiO_2/GCE and Nafion/Hb/Ti_3C_2/GCE with similar procedures as described above. In the control experiment, Nafion/Hb/GCE and Nafion/TiO_2-Ti_3C_2/GCE were also prepared. Before electrochemical measurements, all the as-prepared film electrodes were immersed in pH 7.0 PBS for 30 min to remove residual components.

3. Results and discussions

3.1. Characterization of TiO_2-Ti_3C_2

Fig. 2 shows SEM image of typical as-synthesized Ti_3C_2 (a), TiO_2-Ti_3C_2 nanocomposite (b)-(c), and Nafion/Hb/TiO_2-Ti_3C_2 composite film (d). From Fig. 2(a), the as-synthesized Ti_3C_2 possesses the organ-like structure with one end closing of the Ti_3C_2 nano-layers and the other end opening of that (Wang et al., 2015). And it has a layered morphology resembling exfoliated graphite (Li et al., 2008) and the thickness of the Ti_3C_2 layers is less than 50 nm in average (the inset of Fig. 2(a)). As Fig. 2(b)-(c) shown, after deposition, a lot of TiO_2 nanoparticles (less than 30 nm in size) could be easily loaded on the organ-like Ti_3C_2 layers substrate. And TiO_2 nanoparticles were observed to evenly grow between, and at the edges of the Ti_3C_2 layers (Fig. 2(c)). Note that deposition of TiO_2 with excellent biocompatibility could make TiO_2-Ti_3C_2 nanocomposite have larger specific surface area (approximately 52 m^2 g^{-1}, 2.3 greater than that of the as-synthesized Ti_3C_2, in Fig. S4) and better biocompatibility. Hence, this unique TiO_2-Ti_3C_2 multilayer structure with more inner space could immobilize more Hb and provide a protective microenvironment for the Hb to retain their activity. Fig. 2(d) depicts the microstructure image of Nafion/Hb/TiO_2-Ti_3C_2 composite film. It is noted that TiO_2-Ti_3C_2 is discernible on the surface of modified electrode. TiO_2-Ti_3C_2 was embedded in the Nafion to form a stable composite film, which was essential for the stability of the prepared enzyme electrode. Moreover, because of the high surface area of TiO_2-Ti_3C_2, the effective surface area of the modified electrode improves greatly (Fig. 2(d) and the inset of it).

Fig. S2 presents XRD patterns of Ti_3AlC_2 (curve a), Ti_3C_2 (curve b), and TiO_2-Ti_3C_2 (curve c), respectively. XRD pattern of the HF-etched Ti_3C_2 (curve b), in its air-dried multilayered state, shows

the (00*l*) peaks, such as the (002), (004), and (0010), broadened, lost intensity, and shifted to lower angles compared to their location before treatment (curve a). And the diffraction peaks are in good agreement between the simulated XRD spectra for $Ti_3C_2(OH)_2$ (Naguib et al., 2011). The Ti_3C_2 layers should present suitable surface for ligand interaction, on account of possessing two exposed Ti atoms per unit formula. Since the experiments were conducted in an aqueous environment rich, hydroxyl is the most probable ligand. And the experimental results provides strong evidence of the formation of $Ti_3C_2(OH)_2$, Ti_3C_2 for short. The presence of OH groups was also confirmed by Fourier transform infrared (FTIR) spectroscopy (Fig. S5). Curve c in Fig. S2 exhibited the XRD pattern of the as-prepared TiO_2-Ti_3C_2, all the diffraction peaks are good agreement with that of Ti_3C_2 and the reported JCPDS data of TiO_2 with anatase structure (PDF Card No. 21-1272), which confirms the co-existence of anatase TiO_2 and Ti_3C_2 in the nanocomposite.

3.2. Spectroscopic characterization of Nafion/Hb/TiO_2-Ti_3C_2 composite film

The stability of Hb immobilized on Nafion/Hb/TiO_2-Ti_3C_2 composite film was investigated by UV-vis spectroscopy (Sun et al., 2014a; Sun et al., 2014b). The Soret absorption bands of heme proteins provide information about the conformational integrity of the proteins. As shown in Fig. S6, the Soret absorption band of Hb immobilized on Nafion/Hb/TiO_2-Ti_3C_2 composite film (storage at 4 °C for 60 days) is located at 405.3 nm (curve a), which is close to that of native Hb at 406.2 nm (curve b), indicating the Hb retained the essential features of its conformational integrity. This reveals that TiO_2-Ti_3C_2 nanocomposite has biocompatibility and did not suffer significant protein denaturation.

FTIR spectroscopy is also an effective means to explore the secondary structure of Hb entrapped in Nafion/Hb/TiO_2-Ti_3C_2 composite film (storage at 4 °C for 60 days) (Liu et al., 2015a; Lu et al., 2008; Mao et al., 2014; Sun et al., 2014a). The shapes of amide I and amide II bands of protein provide detailed information on the secondary structure of polypeptide chain (Kauppinen et al., 1981). As shown by the FTIR spectrum of Hb in Fig. S7(B), the amide I band (1700-1600 cm^{-1}) results from C=O stretching vibration of peptide linkages in the backbone of protein. The amide II band (1620-1500 cm^{-1}) is caused by the combination of N–H bending and C–N stretching. As shown in Fig. S7, the spectrum of amide I and II bands of Hb in Hb/TiO_2-Ti_3C_2 composite film (1658 and 1539 cm^{-1}, Fig. S7(A)) are almost the same as that obtained for native Hb (1657 and 1542cm^{-1}, Fig. S7(B)), and are essentially consistent with the reported value of native Hb (Ma and Tian, 2010; Mao et al., 2014; Sun et al., 2013; Sun et al., 2009). The similarities of the two spectra demonstrated that Hb retained the essential features of its native secondary structure on Nafion/Hb/TiO_2-Ti_3C_2 composite film. TiO_2-Ti_3C_2 nanocomposite with good biocompatibility will be a promising matrix for protein immobilization and biosensor fabrication.

3.3. Electrochemical characteristics of the modified electrodes

Fig. 3 shows the typical cyclic voltammograms (CVs) of different modified electrodes in 0.1 M PBS (pH 7.0) at a scan rate of 0.1V s^{-1}. No redox peak is observed at Nafion/TiO_2-Ti_3C_2/GCE (curve a), which indicates Nafion/TiO_2-Ti_3C_2/GCE is electroinactive in the potential window. The Nafion/Hb/TiO_2-Ti_3C_2/GCE (curve e) exhibits a couple of stable and well-defined redox peaks at -

0.369 V and -0.327 V vs. Ag/AgCl, which could be ascribed to direct electron transfer between Hb and the underlying electrode (Sun et al., 2013). The formal potential ($E^{0'} = (E_{p,a}+E_{p,c})/2$) of Hb was -0.348 V vs. Ag/AgCl is in agreement with -0.345 V and -0.353 V vs. Ag/AgCl reported for the Hb($Fe^{III/II}$) redox couple in Hb-ZnO-Nafion (Lu et al., 2008) and Hb-ZnO-MWCNTs-Nafion (Ma and Tian, 2010) films. Compared with that of the Nafion/Hb/TiO_2-Ti_3C_2/GCE, almost no redox peaks observed at the Nafion/Hb/GCE (curve b, in Fig. 3), suggesting an enhanced electron transfer between Hb molecules and the surface of the Nafion/Hb/TiO_2-Ti_3C_2/GCE. Meanwhile, the much smaller redox peaks of Nafion/Hb/GCE can be attributed to the denaturation of proteins on the bare electrode surface and the difficulty for proteins realizing the DET process on the bare electrode (Dong et al., 2011; Zhu et al., 2011). It can be clearly seen from the comparison that direct electron transfer between Hb molecules and GCE is greatly enhanced at the Nafion/Hb/TiO_2-Ti_3C_2/GCE. For comparison, Nafion/Hb/TiO_2/GCE and Nafion/Hb/Ti_3C_2/GCE have also been carried out (curve c and d, in Fig. 3). The redox peaks of the two electrodes are 54.3% (TiO_2) and 21.7% (Ti_3C_2) smaller, respectively, than that of Nafion/Hb/TiO_2-Ti_3C_2/GCE. It can be concluded that TiO_2-Ti_3C_2 nanocomposite has better effect on the facilitation of electron transfer, which may result from unique morphology and property of that.

Fig. S8 shows the cyclic voltammograms of Nafion/Hb/TiO_2-Ti_3C_2/GCE at 0.1 M PBS (pH 7.0) when the scan rate was increased from 0.1 to 0.8 V s^{-1}. With the increase of the scan rate, the cathodic and anodic peak currents of Hb increase simultaneously, meanwhile the cathodic and anodic peak

potentials show a small shift and the peak to peak separation also become slightly enlarged. The inset of Fig. S8 shows that the cathodic (i_{pc}) and anodic (i_{pa}) peak currents increase linearly with scan rates from 0.1 to 0.8 V s^{-1}. This reveals that the electrode reaction corresponds to a surface attached reaction process. Moreover, the slopes of anodic and cathodic processes are nearly equal suggests that Hb is stable and not undergoing denaturation. Using the Laviron method for a surface-controlled electrochemical system (Laviron, 1979), the apparent heterogeneous electron transfer rate constant (k_s) of Hb immobilized on Nafion/TiO_2-Ti_3C_2/GCE is estimated to be about 2.94 s^{-1}, which is higher than the value reported for Hb immobilized TiO_2 nanorods-graphene (0.65 s^{-1}) (Sun et al., 2013), ZnO-MWCNTs (1.14 s^{-1}) (Ma and Tian, 2010) and nitrogen-doped graphene (2.36 s^{-1}) (Sun et al., 2014a), suggesting a faster electron-transfer process. This means that TiO_2-Ti_3C_2 nanocomposite facilitates the direct electron transfer of Hb.

The average surface concentration of electroactive Hb (Γ*, mol cm^{-2}) can be estimated from the charge integration of the reduction peak of the CV using the formula:

$$Q = nFA\Gamma^* \quad (1)$$

where F is Faraday constant, Q is the charge (C) and can be obtained by integrating the reduction peak of Hb, n and A stand for the number of electron transferred and the geometrical surface area of the electrode, respectively. According to this method, the surface concentration of electroactive Hb (Γ*) *at* Nafion/Hb/TiO_2-Ti_3C_2/GCE was calculated as 5.35×10^{-10} mol cm^{-2}, which is much greater than the theoretical value for monolayer coverage (1.89×10^{-11} mol cm^{-2}) (Wang et al., 2005). This means that

multilayer of Hb entrapped in the Nafion/Hb/TiO_2-Ti_3C_2 composite film participated in the electron-transfer process. Meanwhile, the surface concentration of electroactive Hb of Nafion/Hb/TiO_2-Ti_3C_2/GCE is higher than that of Nafion/Hb/Ti_3C_2/GCE (4.37×10^{-10} mol cm^{-2}) (Liu et al., 2015b), revealing that TiO_2-Ti_3C_2 possesses larger specific surface area and better biocompatibility than Ti_3C_2, and can immobilize more Hb and retain its bioactivity and stability on the surface of GCE. And the Γ^* (Hb) of Nafion/Hb/TiO_2-Ti_3C_2/GCE is comparable some graphene-based Hb modified electrodes reported previously (Table S1). This suggests that TiO_2-Ti_3C_2 nanocomposite can immobilize more Hb and retain its activity and stability on the surface of GCE.

Fig. S9 shows the cyclic voltammograms of 0.1 M PBS of different pH values at a Nafion/Hb/TiO_2-Ti_3C_2/GCE. Stable and well-defined CVs were observed in the pH values range 6.0~8.0. With the increase of pH value, both the cathodic and anodic peaks shifted to the negative (Fig. S9). This can be contributed to the involvement of proton transfer in the Hb(Fe^{III})/Hb(Fe^{II}) redox couple (Chen et al., 2015). The $E^{0'}$ value of Hb varied linearly in the range of pH values of 6.0~8.0, with a slop of -52.9 mV pH^{-1} (the inset of Fig. S9). This value is very close to the theoretical value for the transfer of one proton and electron in a reversible reduction (-58mV pH^{-1} at 25 °C) (Chen et al., 2015; Xie et al., 2011).

3.4. Electrocatalytic properties of the Nafion/Hb/TiO_2-Ti_3C_2/GCE

When Hb is immobilized on an electrode surface with retained bioactivity, it usually exhibits electrocatalytic activity for H_2O_2, nitrite and Cl_3CCOOH (Liu et al., 2014; Lu et al., 2008; Sun et al.,

2013; Wang et al., 2010). By using H_2O_2 as a probe, the electrocatalytic properties of the Nafion/Hb/TiO_2-Ti_3C_2/GCE were investigated. As shown in Fig. 4, the reduction peak increased dramatically with the addition of H_2O_2, accompanied by a decrease and disappearance of the oxidation peak, displaying the obvious electrocatalytic behavior of Hb for the reduction of H_2O_2 (Liu et al., 2014; Lu et al., 2008). A possible reaction mechanism of H_2O_2 catalyzed by the Hb-based electrode is postulated as follows (Ferapontova, 2004):

$$Hb(Fe^{III}) + e^- \rightleftharpoons Hb(Fe^{II}) \quad (2)$$

$$Hb(Fe^{II}) + H_2O_2 + 2H^+ \rightarrow Hb(Fe^{III}) + 2H_2O \quad (3)$$

On increasing the H_2O_2 concentration, the current value reached a saturation limit (the inset of Fig. 4), and saturation behavior was characteristic of enzyme-based catalysis. The apparent Michaelis-Menten constant (K_M^{app}) can be obtained by the electrochemical-version of Lineweaver-Burk equation (Kamin and Wilson, 1980):

$$1/I_{ss} = K_M^{app} / (I_{max}\, C) + 1/I_{max} \quad (4)$$

where I_{ss} is the steady-state current after the addition of substrate, C is the bulk concentration of the substrate, and I_{max} is the maximum current measured under saturated substrate conditions. The K_M^{app} value of Nafion/Hb/TiO_2-Ti_3C_2/GCE was estimated to be 86 μM (Fig. S10 (curve a)). This value was smaller than those ever reported values of 180 μM (Dong et al., 2011) and 379 μM (Sun et al., 2012), indicating that Hb immobilized on Nafion/Hb/TiO_2-Ti_3C_2/GCE retained higher bioactivity and had a high biological affinity to H_2O_2. Note that the K_M^{app} value of Nafion/Hb/TiO_2-Ti_3C_2/GCE was also

smaller than that of Nafion/Hb/Ti_3C_2/GCE (95 μM) (Fig. S10 (curve a)), revealing that TiO_2 nanoparticles could enhance the biocompatibility of the Ti_3C_2 MXene-based nanocomposite.

3.5. Biosensor performance of the Nafion/Hb/TiO_2-Ti_3C_2/GCE

The biosensor performance for the detection of H_2O_2 of the Nafion/Hb/TiO_2-Ti_3C_2/GCE was also investigated by amperometry. Fig. 5 gives the amperometric responses of the modified glassy carbon electrodes at −0.35 V after adding H_2O_2 in stirred PBS (pH 7.0). Curve b in Fig. 5(A) demonstrates that, on Nafion/Hb/TiO_2-Ti_3C_2/GCE, the response time (achieving 95% of the steady-state current) was less than 3 s. Moreover, for Nafion/Hb/TiO_2-Ti_3C_2/GCE, a well-defined linear relationship between the current and the H_2O_2 concentration was observed. The calibration plot (curve b in Fig. 5(B)) showed a linear range from 0.1 to 380 μM (correlation coefficient of 0.999, N=32) with a sensitivity of 447.3 μA mM^{-1} cm^{-2} and a detection limit of 14 nM (based on a signal-to-noise ratio of 3). Curve a in Fig. 5(A) shows the amperometric response of the Nafion/Hb/Ti_3C_2/GCE under the same conditions of continuous addition of H_2O_2 to PBS. It can be seen that the Nafion/Hb/Ti_3C_2/GCE yielded a detectable, but relatively smaller current response to H_2O_2. Both of the linear range (0.1~260 μM) (curve a in Fig. 5(B)) and sensitivity (321.7 μA mM^{-1} cm^{-2}) of Nafion/Hb/Ti_3C_2/GCE are weaker than that of Nafion/Hb/TiO_2-Ti_3C_2/GCE. Performances of various H_2O_2 biosensors are listed in Table S2. It is clear that the performance of Nafion/Hb/TiO_2-Ti_3C_2/GCE was significantly improved. Furthermore, in Fig. S11 and Table S3, compared with Nafion/Hb/TiO_2/GCE and Nafion/Hb/GCE, the TiO_2-Ti_3C_2 based biosensor has better performance. There are some reasons why the Nafion/Hb/TiO_2-Ti_3C_2/GC electrode

displays both a lower detection limit and a wider linear range. Firstly, the organ-like TiO_2-Ti_3C_2 hybrid structure provides a favorable microenvironment for the protein to retain its activity and stability. More importantly, the substrate can simply be entrapped by TiO_2-Ti_3C_2 with larger specific surface area and the special organ-like structure, and have easy access to the enzymes immobilized on the surface of TiO_2-Ti_3C_2 nano-layers. There is an increased chance of effective collisions between substrate and redox protein leading to improved performance of this sensor (Xie et al., 2011).

3.6. Selectivity of the H_2O_2 biosensor

Selectivity is important in practical use of the biosensors, and the selectivity of the biosensor was evaluated with four typical interfering substances (glucose (Glu), dopamine (DA), uric acid (UA) and ascorbic acid (AA)) by using the amperometric current-time method. As Fig. S12 shown, four tested substances did not interfere significantly with the resulting biosensor. This result might be attributed to the intrinsic selectivity of Hb for its substances.

3.7. Stability and reproducibility of the biosensor

The stability of the Nafion/Hb/TiO_2-Ti_3C_2/GCE is investigated with two methods. Firstly, 100 continuous cyclic scans on Nafion/Hb/TiO_2-Ti_3C_2/GCE were repeated in the potential range from -0.7 V to 0.1 V with a scan rate of 0.1 V s^{-1} (Fig. S13). There was nearly no decrease of the voltammetric response and 96.3% of the initial current response was retained. Hence, the prepared Nafion/Hb/TiO_2-Ti_3C_2/GCE possesses excellent cycle stability. Meanwhile, the long-term stability is an important evaluation index for estimating the performance of biosensor. The long-term stability of fabricated

biosensor was studied by examining its current response. When not in use, the fabricated biosensor was stored dry at 4 °C. The biosensor retained about 97.5% of its initial response to H_2O_2 after 30 days and 94.6% after 60 days, demonstrating good long-term stability (Fig. 6). Additionally, compared with that of Nafion/Hb/TiO_2-Ti_3C_2/GCE, the stability of Nafion/Hb/Ti_3C_2/GCE is relatively worse (Fig. S13 and Fig. 6). The good stability can be contributed to the good biocompatibility of TiO_2-Ti_3C_2 nanocomposite, which can provide a favorable microenvironment for Hb to retain its bioactivity.

The reproducibility of the biosensor was investigated by determining 4 μM H_2O_2 in PBS (pH 7.0). The relative standard deviation (R.S.D) was 2.1% respectively for 5 successive measurements. Five biosensors prepared under the same conditions independently gave a R.S.D. of 2.6% for the determination of 4 μM, indicating an acceptable electrode-to-electrode reproducibility.

3.8. Analysis of real samples

In order to evaluate the analytical utility of the electrode in practice, the Nafion/Hb/TiO_2-Ti_3C_2/GCE was applied for determination of disinfector samples (3.0% H_2O_2). Before experiments, the real samples were diluted 5000 times with doubly distilled water and without any other pretreatment. Recovery tests and $KMnO_4$ titration method were used to examine the reliability and accuracy of this method. The H_2O_2 content of different samples and recoveries of added analyte were evaluated, and the results confirmed that it is possible to determine the H_2O_2 concentration in real samples using the proposed method (Table S4).

4. Conclusion

TiO_2 nanoparticle modified Ti_3C_2 MXene nanocomposite has been synthesized through a simple synthetic route, and subsequently used to fabricate a mediator-free biosensor for the detection of H_2O_2. The special organ-like structure of TiO_2-Ti_3C_2 nanocomposite not only could be beneficial to immobilize more Hb but also could simply entrap the substrate. Hence, there is an increased chance of effective collisions between substrate and redox protein leading to improved performance of this sensor. More importantly, numerous TiO_2 nanoparticles with excellent biocompatibility on the surface of the nanocomposite may provide a protective microenvironment for Hb to retain its bioactivity and stability for long time. Due to the above reasons, the prepared biosensors displayed a low detection limit of 14 nM, a wide linear range of 0.1-380 μM for H_2O_2, and especially, an excellent long-term stability. This study indicates that TiO_2-Ti_3C_2 nanocomposite can be used as biocompatible matrix for the enzyme immobilization and the construction of direct electrochemical biosensor.

Acknowledgments

This work was supported by the National Natural Science Foundation of China (51472153, 51171096), and the Graduate Innovation Fund of Shaanxi University of Science and Technology.

References

Armstrong, F.A., Hill, H.A.O., Walton, N.J., 1988. Acc. Chem. Res. 21 (11), 407-413.

Chen, X., Wang, Q., Wang, L., Gao, F., Wang, W., Hu, Z., 2015. Biosens. Bioelectron. 66, 216-223.

Dong, S., Zhang, P., Liu, H., Li, N., Huang, T., 2011. Biosens. Bioelectron. 26 (10), 4082-4087.

Elahi, M.Y., Khodadadi, A.A., Mortazavi, Y., 2014. J. Electrochem. Soc. 161 (5), B81-B87.

Ferapontova, E.E., 2004. Electroanalysis 16 (13-14), 1101-1112.

Heller, A., 1990. Acc. Chem. Res. 23 (5), 128-134.

Hong, J., Ghourchian, H., Moosavi–Movahedi, A.A., 2006. Electrochem. Commun. 8 (10), 1572-1576.

Jain, R., Sharma, R., Yadav, R.K., Shrivastava, R., 2013. J. Electrochem. Soc. 160 (3), H179-H184.

Jin, M., Zhang, X., Nishimoto, S., Liu, Z., Tryk, D.A., Emeline, A.V., Murakami, T., Fujishima, A., 2007. J. Phys. Chem. C 111 (2), 658-665.

Kamin, R.A., Wilson, G.S., 1980. Anal. Chem. 52 (8), 1198-1205.

Kauppinen, J.K., Moffatt, D.J., Mantsch, H.H., Cameron, D.G., 1981. Appl. Spectrosc. 35 (3), 271-276.

Laviron, E., 1979. J. Electroanal. Chem. Interfac. 101 (1), 19-28.

Li, X., Wang, X., Zhang, L., Lee, S., Dai, H., 2008. Science 319 (5867), 1229-1232.

Liu, H., Duan, C., Su, X., Dong, X., Huang, Z., Shen, W., Zhu, Z., 2014. Sens. Actuators B: Chem. 203, 303-310.

Liu, H., Duan, C., Yang, C., Chen, X., Shen, W., Zhu, Z., 2015a. Mater. Sci. Eng., C 53, 43-49.

Liu, H., Duan, C., Yang, C., Shen, W., Wang, F., Zhu, Z., 2015b. Sens. Actuators B: Chem. 218, 60-66.

Lu, X., Hu, J., Yao, X., Wang, Z., Li, J., 2006. Biomacromolecules 7 (3), 975-980.

Lu, X., Zhang, H., Ni, Y., Zhang, Q., Chen, J., 2008. Biosens. Bioelectron. 24 (1), 93-98.

Ma, L., Yuan, R., Chai, Y., Chen, S., 2009. J. Mol. Catal. B: Enzym. 56 (4), 215-220.

Ma, W., Tian, D., 2010. Bioelectrochemistry 78 (2), 106-112.

Mao, Q.-X., Wang, H., Shu, Y., Chen, X.-W., Wang, J.-H., 2014. RSC Adv. 4 (16), 8177-8182.

Naguib, M., Kurtoglu, M., Presser, V., Lu, J., Niu, J., Heon, M., Hultman, L., Gogotsi, Y., Barsoum, M.W., 2011. Adv. Mater. 23 (37), 4248-4253.

Naguib, M., Mochalin, V.N., Barsoum, M.W., Gogotsi, Y., 2014. Adv. Mater. 26 (7), 992-1005.

Peng, Q., Guo, J., Zhang, Q., Xiang, J., Liu, B., Zhou, A., Liu, R., Tian, Y., 2014. J. Am. Chem. Soc. 136 (11), 4113-4116.

Qiu, J., Peng, H., Liang, R., Xia, X., 2010. Biosens. Bioelectron. 25 (6), 1447-1453.

Scheller, F.W., Bistolas, N., Liu, S., Janchen, M., Katterle, M., Wollenberger, U., 2005. Adv. Colloid Interface Sci. 116 (1-3), 111-120.

Sun, A., Zhao, H., Zheng, J., 2012. Talanta 88, 259-264.

Sun, W., Dong, L., Deng, Y., Yu, J., Wang, W., Zhu, Q., 2014a. Mater. Sci. Eng., C 39, 86-91.

Sun, W., Gong, S., Shi, F., Cao, L., Ling, L., Zheng, W., Wang, W., 2014b. Mater. Sci. Eng., C 40, 235-241.

Sun, W., Guo, Y., Ju, X., Zhang, Y., Wang, X., Sun, Z., 2013. Biosens. Bioelectron. 42, 207-213.

Sun, W., Zhai, Z., Wang, D., Liu, S., Jiao, K., 2009. Bioelectrochemistry 74 (2), 295-300.

Wang, F., Yang, C., Duan, C., Xiao, D., Tang, Y., Zhu, J., 2015. J. Electrochem. Soc. 162 (1), B16-B21.

Wang, G., Shen, X., Wang, B., Yao, J., Park, J., 2009. Carbon 47 (5), 1359-1364.

Wang, S.-F., Chen, T., Zhang, Z.-L., Shen, X.-C., Lu, Z.-X., Pang, D.-W., Wong, K.-Y., 2005. Langmuir 21 (20), 9260-9266.

Wang, Y., Ma, X., Wen, Y., Xing, Y., Zhang, Z., Yang, H., 2010. Biosens. Bioelectron. 25 (11), 2442-2446.

Xiao, J., Choi, D., Cosimbescu, L., Koech, P., Liu, J., Lemmon, J.P., 2010. Chem. Mater. 22 (16), 4522-4524.

Xie, Q., Zhao, Y., Chen, X., Liu, H., Evans, D.G., Yang, W., 2011. Biomaterials 32 (27), 6588-6594.

Xie, Y., Zhou, L., Huang, H., 2007. Biosens. Bioelectron. 22 (12), 2812-2818.

Zhang, L., Zhang, Q., Lu, X., Li, J., 2007. Biosens. Bioelectron. 23 (1), 102-106.

Zhu, Z., Qu, L., Niu, Q., Zeng, Y., Sun, W., Huang, X., 2011. Biosens. Bioelectron. 26 (5), 2119-2124.

Figure Captions:

Figure 1. Schematic illustration of the organ-like structure of TiO_2-Ti_3C_2 nanocomposite encapsulating hemoglobin.

Figure 2. SEM images of typical as-synthesized Ti_3C_2 (a), TiO_2-Ti_3C_2 nanocomposite (b)-(c), and Nafion/Hb/TiO_2-Ti_3C_2 composite film (d).

Figure 3. Cyclic voltammograms of Nafion/TiO_2-Ti_3C_2/GCE (curve a), Nafion/Hb/GCE (curve b), Nafion/Hb/TiO_2/GCE (curve c), Nafion/Hb/Ti_3C_2/GCE (curve d), Nafion/Hb/TiO_2-Ti_3C_2/GCE (curve e) in 0.1M pH 7.0 PBS with a scan rate of 0.1 V s^{-1}.

Figure 4. Cyclic voltammograms of Nafion/Hb/TiO_2-Ti_3C_2/GCE in 0.1 M pH 7.0 PBS containing 0 (a), 10 (b), 30 (c), 50 (d), 70 (e), 110 (f), 150 (g), 190 (h), 230 (i), 310 (j) H_2O_2 with a scan rate of 0.1 V s^{-1}. Inset: plot of the cathodic peak current vs. H_2O_2 concentration: Nafion/Hb/Ti_3C_2/GCE (curve a) and Nafion/Hb/TiO_2-Ti_3C_2/GCE (curve b).

Figure 5. (A) Typical current-time response of Nafion/Hb/Ti_3C_2/GCE (curve a) and Nafion/Hb/TiO_2-Ti_3C_2/GCE (curve b) at -0.35V to successive addition of H_2O_2 in stirred 0.1 M pH 7.0 PBS. (B) The steady state current vs. H_2O_2 concentration: Nafion/Hb/Ti_3C_2/GCE (curve a) and Nafion/Hb/TiO_2-Ti_3C_2/GCE (curve b).

Figure 6. Cyclic voltammograms of Nafion/Hb/TiO_2-Ti_3C_2/GCE (A) and Nafion/Hb/Ti_3C_2/GCE (B) in 0.1 M pH 7.0 PBS containing 100 μM H_2O_2 on the first day (a), 30^{th} day (b) and 60^{th} day (c) after the preparation. Scan rate: 100 mV s^{-1}. (C) The relationship between the cathodic peak current

and the storage time.

Figure 1.

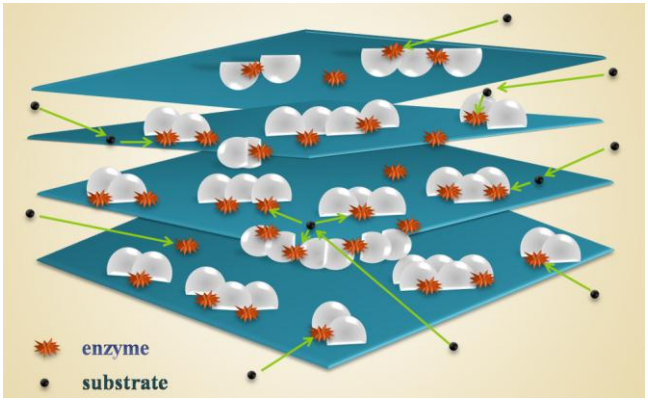

Figure 1. Schematic illustration of the organ-like structure of TiO_2-Ti_3C_2 nanocomposite encapsulating hemoglobin.

Figure 2.

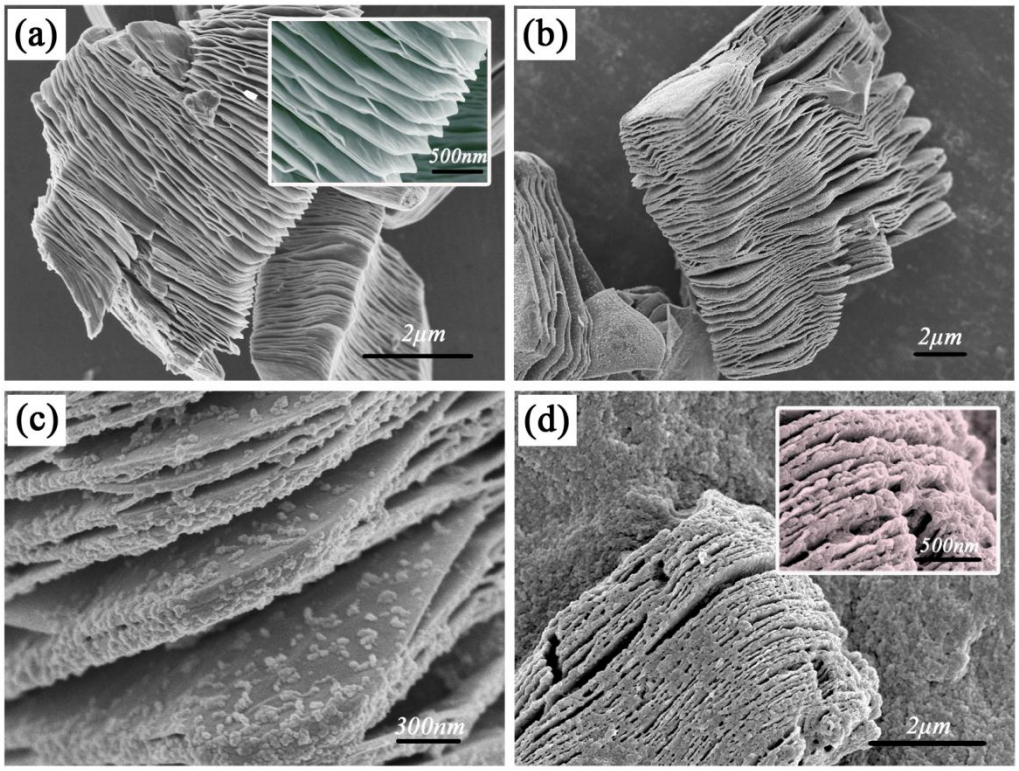

Figure 2. SEM images of typical as-synthesized Ti_3C_2 (a), TiO_2-Ti_3C_2 nanocomposite (b)-(c), and Nafion/Hb/TiO_2-Ti_3C_2 composite film (d).

Figure 3.

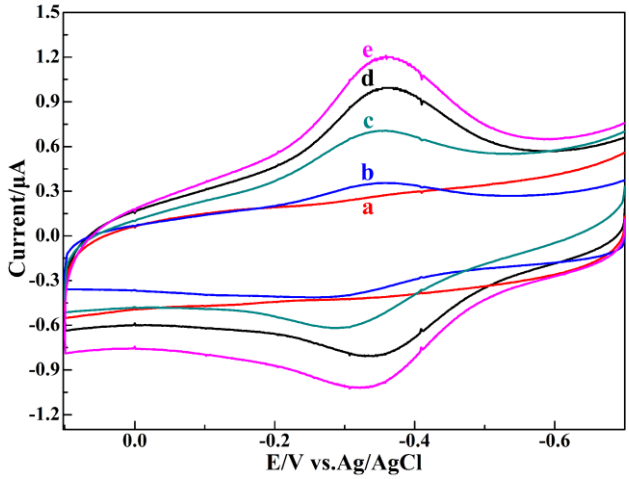

Figure 3. Cyclic voltammograms of Nafion/TiO_2-Ti_3C_2/GCE (curve a), Nafion/Hb/GCE (curve b), Nafion/Hb/TiO_2/GCE (curve c), Nafion/Hb/Ti_3C_2/GCE (curve d), Nafion/Hb/TiO_2-Ti_3C_2/GCE (curve e) in 0.1M pH 7.0 PBS with a scan rate of 0.1 V s^{-1}.

Figure 4.

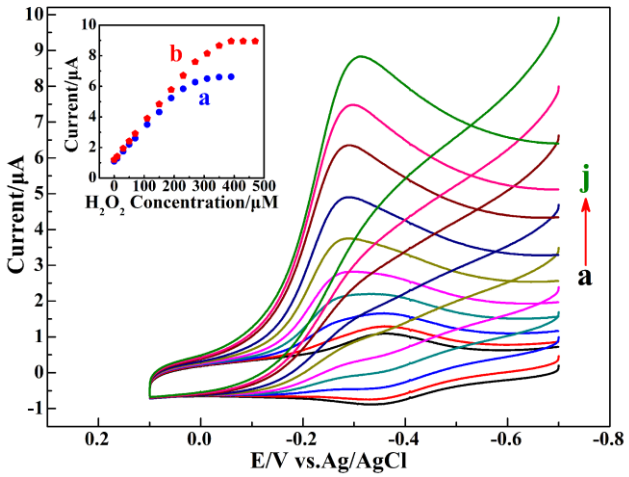

Figure 4. Cyclic voltammograms of Nafion/Hb/TiO_2-Ti_3C_2/GCE in 0.1 M pH 7.0 PBS containing 0 (a), 10 (b), 30 (c), 50 (d), 70 (e), 110 (f), 150 (g), 190 (h), 230 (i), 310 (j) H_2O_2 with a scan rate of 0.1 V s^{-1}. Inset: plot of the cathodic peak current vs. H_2O_2 concentration: Nafion/Hb/Ti_3C_2/GCE (curve a) and Nafion/Hb/TiO_2-Ti_3C_2/GCE (curve b).

Figure 5.

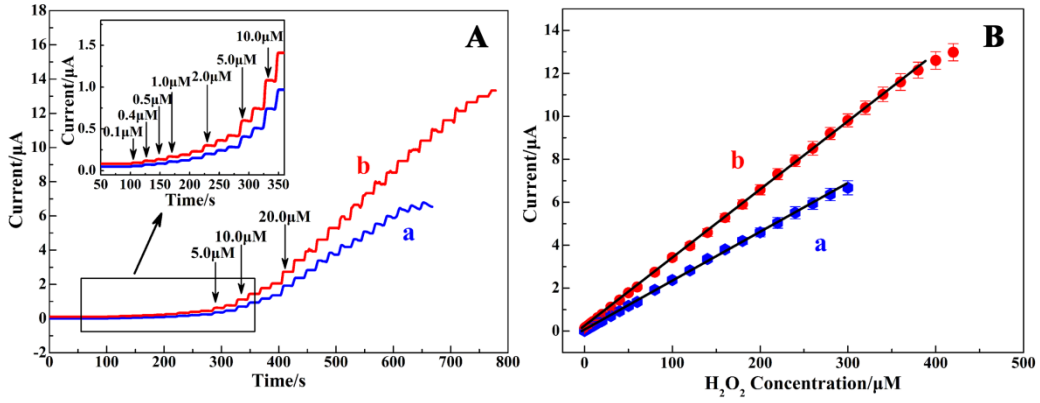

Figure 5. (A) Typical current-time response of Nafion/Hb/Ti_3C_2/GCE (curve a) and Nafion/Hb/TiO_2-Ti_3C_2/GCE (curve b) at -0.35V to successive addition of H_2O_2 in stirred 0.1 M pH 7.0 PBS. (B) The steady state current vs. H_2O_2 concentration: Nafion/Hb/Ti_3C_2/GCE (curve a) and Nafion/Hb/TiO_2-Ti_3C_2/GCE (curve b).

Figure 6.

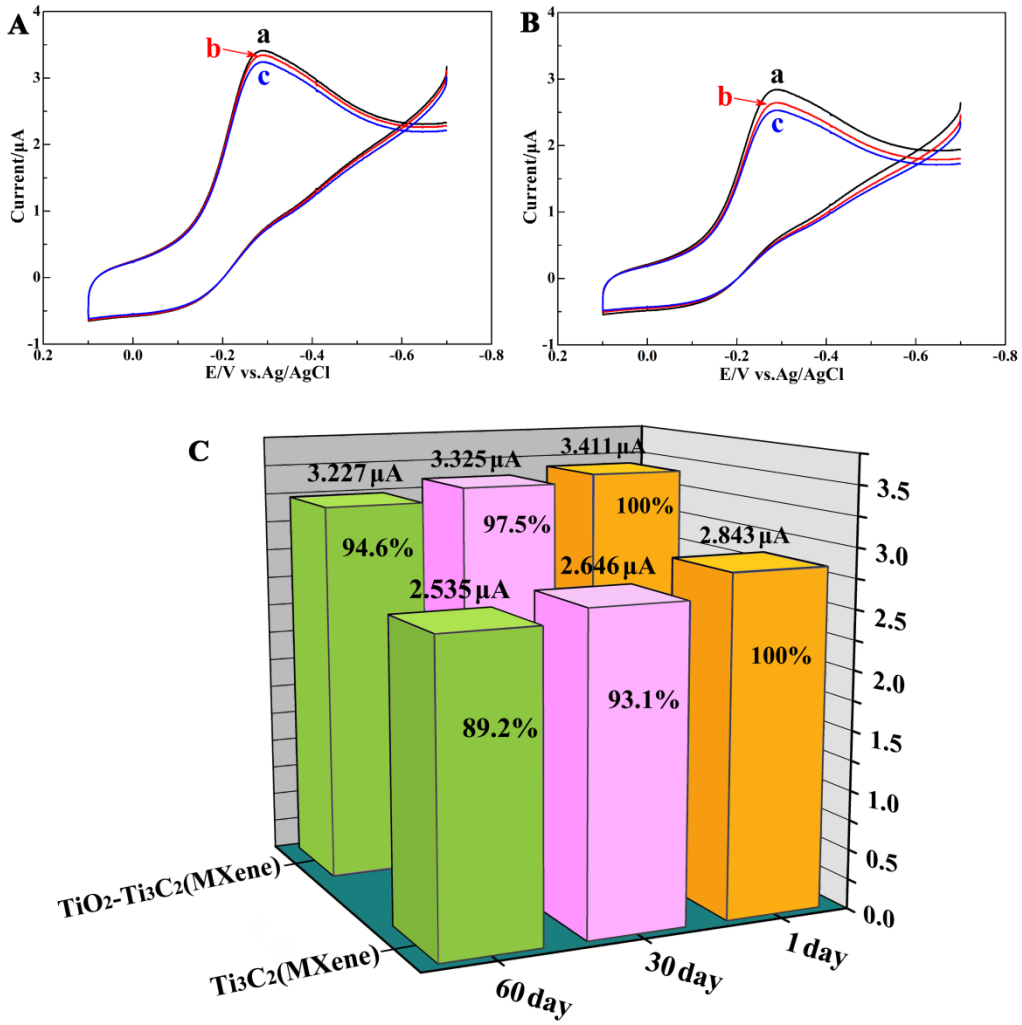

Figure 6. Cyclic voltammograms of Nafion/Hb/TiO_2-Ti_3C_2/GCE (A) and Nafion/Hb/Ti_3C_2/GCE (B) in 0.1 M pH 7.0 PBS containing 100 μM H_2O_2 on the first day (a), 30^{th} day (b) and 60^{th} day (c) after the preparation. Scan rate: 100 mV s^{-1}. (C) The relationship between the cathodic peak current and the storage time.

Highlights

- A novel TiO_2-Ti_3C_2 nanocomposite with excellent biocompatibility has been synthesized.
- TiO_2-Ti_3C_2 nanocomposite is used to fabricate a mediator-free biosensor firstly.
- The biosensor displays a wide linear range of 0.1-380 μM for H_2O_2.
- The biosensor exhibits a low detection limit of 14 nM for H_2O_2.
- Especially, the biosensor possesses an excellent long-term stability.

Graphical Abstract